

Characterisation of interfaces in nanocrystalline palladium

R DIVAKAR and V S RAGHUNATHAN

Physical Metallurgy Section, Materials Characterisation Group, Indira Gandhi
Centre for Atomic Research, Kalpakkam 603 102, India
e-mail: divakar@igcar.ernet.in

Abstract. Structures of grain boundaries and triple line junctions in nanocrystalline materials are of interest owing to large fractions of atoms in nanocrystalline materials being at these interfacial positions. Grain boundary and triple line junction structures in nanocrystalline palladium have been studied using high-resolution transmission electron microscopy (HRTEM). The main microstructural features observed include the varying atomic structures of grain boundaries and the presence of disordered regions at triple line junctions. Also, there is variation in lattice parameters in different nanocrystalline grains. Geometric phase analysis is used to quantify atomic displacements within nanocrystalline grains. Displacement fields thus detected indicate links to the interface structures.

Keywords. Nanocrystalline palladium; HRTEM; interfaces; grain boundaries; triple line junctions.

1. Introduction

Nanocrystalline materials are crystalline aggregates limited spatially in one or more dimensions to nanometre scales. The landmark lecture by Feynman (1960) is most often quoted as the beginning of nanoscience research. These materials were, however, not synthesised until the early 1970s by Gleiter and co-workers. These materials are a subset of the broader class of nanostructured materials, which include materials with microstructural constituents at the nanometre scale in zero to three dimensions, as clusters, multilayers, ultrafine grained surface overlays and bulk nanophase materials. A review of nanostructured materials is presented by Gleiter (2000). In the present paper, experimental results from high-resolution transmission electron microscopy (HRTEM) of nanocrystalline palladium thin films are presented after a brief review of the study of nanocrystalline materials and the interfaces therein.

At the small grain sizes seen in nanocrystalline materials, most physical properties show significant deviations from corresponding values for the same material with coarser grain sizes, primarily because of two factors. The first is the result of the interaction of two length scales: Characteristic lengths of the physical phenomena and of the microstructure (Arzt 1998). The microstructural characteristic length can be the grain size or the grain boundary width depending upon the nature of the physical phenomena involved. Physical properties that can be correlated to such a characteristic length scale show marked deviations from bulk properties when the characteristic length becomes comparable to the grain size or a related parameter. For example, in the case of single-phase magnetic materials, interesting effects are seen when the

grain size reduces to the magnetic domain wall width (Löffler *et al* 2000). Similarly, deviation from the Hall–Petch relation observed for nanocrystalline materials (Nieh & Wadsworth 1991) is due to the finite number of dislocations in a pile-up. The Hall–Petch relation presumes dislocation pile-ups consisting of a large number of dislocations while below a certain grain size, even two dislocations may not be able to exist on the same slip plane.

Second, the fraction of atoms at grain boundary positions becomes significant. As a first approximation, consider a spherical grain of diameter d with a concentric shell of thickness δ as the grain boundary part. Volume of this boundary as a fraction of the total grain volume is

$$v = \frac{4\pi(d/2)^2\delta}{(4/3)\pi(d/2)^3} = \frac{6\delta}{d}. \quad (1)$$

According to this simplistic model, grain boundary volume fraction is as much as 50% for a grain size of ≈ 6 nm, assuming a grain boundary thickness value of 0.5 nm. This simplistic relation is an overestimate and yields unrealistic results when $d \leq \delta$. A more realistic model based on regular tetrakaidecahedral (14-faced) grains (Palumbo *et al* 1990) indicates that the 50% volume fraction for the inter-crystalline regions is at 2.4 nm with the triple line junctions forming a significant 20% of the inter-crystalline volume fraction. Figure 1 shows the variation of the grain boundary volume fraction as a function of the grain size for the sphere model as well as the tetrakaidecahedral model. At conventional grain sizes of the order of a few microns, the corresponding fraction is well under 1%. Beginning at grain sizes smaller than ≈ 50 nm, where the grain boundary volume fraction exceeds a few percent, we can expect to see deviations in physical properties. The actual grain size range where deviations become significant depends on the nature of the physical phenomena involved. The atomic configuration at the grain boundaries and triple line junctions is of significant interfacial phenomena such as solid state amorphisation reactions (SSAR) where the nanocrystalline state has been suggested to be an essential precursor (Sundaraman 1995). It is also important for physical, chemical, thermal and mechanical properties.

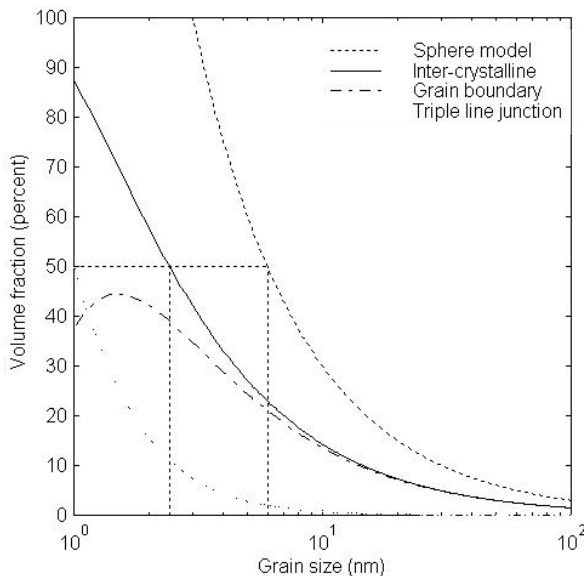


Figure 1. Volume fraction of atoms at interfaces in nanocrystalline materials as calculated based on the simplistic sphere model and the more realistic tetrakaidecahedral grains as given by Palumbo *et al* (1990). The latter set of curves shows that at very small grain sizes, the grain boundary and triple line junction fractions are of comparable magnitude. The grain size corresponding to 50% volume fraction of interfacial atoms is indicated.

Interface structures in nanocrystalline materials have been the subject of research from the very beginning. The first indication that the structure of grain boundaries in nanocrystalline materials was different was from the X-ray diffraction (XRD) studies of Zhu *et al* (1987) on nanocrystalline Fe. A large diffuse background in computed and experimental XRD patterns was interpreted to indicate that the interfacial regions lacked either short range or long range order. Haubold *et al* (1989) concluded from their Extended X-ray Absorption Fine Structure (EXAFS) investigation of nanocrystalline palladium and copper that the grain boundary component of these nanocrystalline materials has random atomic arrangements similar to 'gas-like' disorder. The basic idea used was that only the crystalline component contributes to the EXAFS oscillations and that materials with random atomic arrangements result in no oscillations of the EXAFS signal. Analysis of the EXAFS signal was according to the method of Lengeler & Eisenberger (1980). The chief feature of the results was that the amplitude of the signal corresponding to the first co-ordination shell was reduced by a fraction comparable to the volume fraction of grain boundaries in the nanocrystalline materials. However, HRTEM studies of Thomas *et al* (1990) did not find disorder at grain boundaries that could be called 'gas-like' disorder and that the grain boundary structure is not fundamentally different from that in conventional polycrystalline coarse-grained materials. The observed contrast changes at grain boundaries could be due to a number of other reasons: vacancies, ultrafine porosity, atomic relaxation and impurity segregation. The contrast change at grain boundaries was reported to be localised to within 0.4 nm. Wunderlich *et al* (1990) reported in their HRTEM study of the microstructure of nanocrystalline palladium voids in the size range 0.1–1 nm. They also reported that while the triple line junctions are usually 'filled' with atoms in crystalline order, voids are sometimes observed and rarely are amorphous regions observed. Fitzsimmons *et al* (1991) concluded from their XRD studies on 7–20 nm palladium nanocrystals that the diffuse background does not significantly differ from coarse grained materials and thus offers no evidence for the lack of short-range or long-range order at grain boundaries. The EXAFS and hydriding studies of Eastman *et al* (1992) on nanocrystalline palladium further confirmed this. A number of investigations by HRTEM of the structure of nanocrystalline materials have since been reported. Li *et al* (1993) observed that the grain boundaries have ordered as well as disordered regions in addition to nanovoids. Other features such as five-fold twins have also been reported. Ping *et al* (1995b) have recognised that differences in microstructure, including atomic structures of interfaces could be attributed to the different processing techniques used in the preparation of the nanocrystalline materials. Grain boundaries in nanocrystalline materials have both ordered and disordered regions (Ranganathan *et al* 2000) and lattice fringes near interfaces in nanocrystalline palladium show curved and distorted appearance (Ping *et al* 1995a). This latter fact of distorted lattice fringes should however be considered carefully since they could arise out of many other reasons related to the orientation and imaging conditions of the microscope, as described later. It was generally accepted that the intra-crystalline regions are defect free for grain sizes below a certain material dependant limit. However, no analysis was reported regarding strain in the lattices until recently (Weissmüller 2001).

As the nanocrystalline material grain size decreases, the fraction of atoms at triple line junctions of the total atoms at intercrystalline positions also increases rapidly so as to be of magnitude comparable to the fraction at grain boundaries. Triple line junctions are known to play a role in physical phenomena. Hence the structure at the triple line junction is of special interest in nanocrystalline materials. However, few studies have been devoted to the elucidation of the structure at triple line junctions. The triple line junction structure has been related to a disclination (Bollmann 1988). These triple line junction disclinations may be

classified as balanced I-line or unbalanced U-line disclinations. A number of mechanisms can result in disclinations at triple line junctions in nanocrystalline materials including sequential twinning as in pentagonal nanocrystallites (Melmed & Hayward 1959; Schwobel 1966). Various physical effects have been ascribed to the presence of U-line disclinations at triple line junctions. However, no detailed study of the state of order at triple line junctions has been reported.

2. Materials and experimental techniques

Palladium thin films were prepared by physical vapour deposition (PVD) by resistance heating the palladium in an vacuum coater. Source to substrate distance was about four centimetres. High purity palladium was vaporised by a resistance heater in an Edwards vacuum coater and deposited onto a NaCl crystal. Palladium film coated on NaCl was collected onto 200 mesh, 3 mm diameter copper grids after cutting into square pieces and floating on double distilled water. Thickness of deposition could be well controlled in the 10-30 nm range. Thinner films were preferred to minimise grain overlap in the foil normal direction.

A number of techniques are sensitive to interface structures, requiring varying degrees of data analysis and interpretation. X-ray and neutron scattering experiments are indirect probes of the interfacial structure. They require a fair degree of modelling of the materials' structure including structure of grain boundaries in order to match experimental results and derive useful conclusions regarding interface structure. The signal obtained from these techniques represent a sample average and cannot be used to determine the relative contributions of disorder at grain boundaries and triple line junctions. Compared to these, the phase contrast microscopy technique used in a high-resolution transmission electron microscope (HRTEM) is a direct imaging technique subject to certain imaging conditions being satisfied. HRTEM has been the technique of choice for many interface structure studies. The currently achievable resolution limit of ≈ 0.1 nm by the HRTEM technique is limited worldwide to a few atomic resolution microscopes operated at high voltages. More routinely, a resolution of ≈ 0.2 nm can be achieved at 200 kV, which is adequate for interface imaging in many crystalline systems along low-index zone axes. For the present study, HRTEM was carried out on such a microscope, a 200 kV JEOL 2000 EX II equipped with a top entry stage and an objective lens of spherical aberration coefficient of 0.7 mm and a point resolution of 0.2 nm. A Synergy framestore combined with the Semper image processing software was used for image acquisition and processing. Image simulations were carried out using the multislice technique as implemented in the EMS image simulation package (Stadelman 1987).

In applying the HRTEM technique to interface studies, it is important that two limitations of the technique are taken into account. Firstly, the study of interfaces in the HRTEM requires the orientation of the interface exactly edge-on with the two grains forming the interface along a low index zone axis. Further, the HRTEM technique is insensitive to atomic displacements along the beam direction. This limits the interfaces that can be successfully imaged in polycrystalline materials, but is particularly overcome by using engineered interfaces in grown bicrystals or in the case of randomly oriented nanocrystalline phases. In the latter case, the large number of grain orientations (in the absence of significant texture effects) ensures that interfaces with suitable orientation are available for study. However, it should be noted that it is not possible to image all types of interfaces by HRTEM.

A further objection to HRTEM data used to be that thin foil relaxation effects in the HRTEM specimen preclude use of data to model bulk materials and phenomena. Based

on the HRTEM investigations of interfaces and comparison with simulations in the case of large angle boundaries, it is now felt that thin foil effects are not important, at least for high angle grain boundaries in conventional polycrystalline coarse-grained materials (Mills 1993). Thomas *et al* (1990) have shown that it is possible to identify grain boundary disorder in nanocrystalline materials by the HRTEM technique through combined molecular dynamics and HRTEM images simulations. However, detailed simulations are required to examine the significance of thin foil effects in other cases.

Most materials science studies using HRTEM are carried out for characterisation of some deviation from an ideal structure, be it a defect or an interface. In these, it is useful to get a quantitative picture of the lattice displacements from the ideal positions. If the HRTEM image contrast is a true representation of the specimen structure, there are several techniques for the quantification of atomic displacements. Wood *et al* (1984) have used a direct measurement of lattice fringe displacements for the quantification of the rigid body displacements at grain boundaries. Other techniques to detect lattice distortions include comparison with distortion free lattices derived from the same experimental image or from models to produce moiré patterns as a graphical representation of the lattice distortion. The small grain sizes and the extent of distortion fields preclude such comparisons in the present case of nanocrystalline palladium. Hence, the analysis of lattice structure of the nanocrystalline materials seen in the HRTEM has been carried out in terms of the lattice fringe spacing and the atomic displacements from ideal structure in the nanocrystalline grains. The first and simplest method is by direct measurement in the real space from a HRTEM negative. The advantage of the technique is in its simplicity. However, measurements are time consuming and automating the process is complicated. Alternatively, it is possible to calculate power spectrum from each of the nanocrystalline grains in images scanned or recorded online using a framestore. Peak detection algorithms can then be applied to detect peak positions corresponding to the lattice periodicity in the grain. Advantages are that the process can be made semi-automatic and thus result in a large reduction of labour involved, thus improving repeatability.

Application of these methods can be tedious and requires user intervention and judgement, introducing a factor of subjectivity into the quantification. A better alternative is the geometric phase analysis (GPA) technique (Divakar *et al* 2000). HRTEM lattice or structure images of crystalline materials consist of a periodic array of 1-dimensional or 2-dimensional fringes. The corresponding Fourier transform (FT) then consists of a discrete set of Bragg peaks that can be visualised in the power spectrum. The location of a peak in the FT corresponds to the periodicity and orientation of the fringes in the image, while the phase of the Bragg peak corresponds to the localisation of the fringes in the real space image. The FT can be selectively filtered at Bragg peak locations to extract specific periodicity related information from the image. This involves applying a suitably designed mask to the FT and inverse transforming the filtered transform. The mask design decides the nature of the information obtained. When applied to the FT symmetrically around the origin, information relating to a specific spatial frequency can be extracted while the directionality of the periodicity is lost. Selection of an asymmetric region of the FT gives directional information. GPA involves location specific filtering of the FT. This technique has been used to obtain maps of atomic displacements in a number of experimental situations including semiconductor quantum dots and nanocrystalline grains. The algorithm has been described in detail by Divakar *et al* (2000).

In carrying out these quantification steps on HRTEM images, several precautions in the selection of nanoparticles for quantification of lattice spacings were considered. Image contrast obtained in the HRTEM is directly related to the specimen structure only under strict imaging conditions, and is very sensitive to a number of specimen and microscope parameters.

Further, only lattice images of nanocrystalline materials can be obtained from the HRTEM technique since the diffraction conditions cannot be precisely selected for any or all nanocrystallites. In this context, it is necessary to examine the correspondence of the observed characteristics of the lattice images mentioned above to the actual state of lattice relaxation in nanocrystalline materials. This is especially important for deducing quantitative information such as lattice strain from HRTEM lattice images.

As described above, lattice spacing variations can be measured in the image space by line sections taken along directions perpendicular to the set of planes. Alternatively, variations in spot co-ordinates in the power spectrum from individual grains can be measured. The former technique is useful in recording lattice spacing variations at varying distances from, say, the grain centre, while the latter technique can be used to get an average value over a single grain or several grains. The significance of results from either technique improves as the signal to noise ratio (S/N) is higher in the recorded or scanned image and consequently in the calculated power spectrum. In general, nanograins with 'bent' lattice planes or with poor contrast are not good candidates for such quantification. In small nanoparticles, the length of an atomic column varies from the centre of the grain to the edge. This can give rise to curved lattice planes when tilted off the zone axis. In addition, overlap of the top of an atomic column with the bottom of an adjacent column can give rise to fringe patterns that deceptively mimic lattice spacing. Malm & O'Keefe (1997) have simulated images of a 561-atom palladium nanoparticle over a large range of tilts and have shown that such image artefacts can appear at large tilts away from a low-index zone axis.

Additionally, the measured lattice spacings are sensitive to orientation. For grains that are tilted away from the ideal zone axis, this could be more than 10% away from the true spacing for the set of lattice planes. The power spectrum is an essential indicator of the accuracy of the measured spacing. All measurements in this work were done on grains that gave a power spectrum with a good signal to noise ratio. In cases where cross grating of lattice fringes were obtained, the power spectrum angles and distance ratio can be matched to the expected zone axis. Accuracy is improved by measuring on a large number of grains. For smaller 3 nm grains, accuracy of the order 1% has been estimated (Crozier *et al* 1999). In the present study, the grain sizes are higher, which implies a better sampling in the reciprocal space leading to higher signal to noise ratios. Thus, accuracy of the order 1% corresponding to 0.001 nm is obtained with a smaller number of measurements. Hence, an examination of the power spectrum to confirm good orientation as well as signal to noise ratio, is useful.

With the GPA technique, two additional aspects to be investigated are the phase sampling errors and the effect of the phase changes due to foil thickness as well as defocus. Arbitrary sampling of the displacement image will lead to difficulties in the interpretation of the results. There are two possible approaches. The first, which has been adopted in the present work, uses the reciprocal lattice vectors to determine the real space lattice vectors. The origin of the real space lattice is then chosen and a real space lattice is defined. The phase image is then sampled at the resulting lattice points. The alternative approach is to use peak finding routines to identify the atom positions in the real image. The displacement images corresponding to two non-collinear reciprocal lattice reflections are then sampled at these points to yield the quiver plot of atomic displacements. Relative merits of these two approaches are being examined and will be reported elsewhere. To evaluate the effect of sample thickness and defocus, image simulations were carried out using multislice technique. A super-cell consisting of several unit cells of a *fcc* structure was constructed. A distortion field was introduced into this lattice. As a preliminary approximation, a radial distortion field has been chosen. Images were simulated for various crystal thicknesses along the beam direction and several defocus steps. Thickness

values were chosen to approximate the thin film thickness examined experimentally. Defocus values around the Scherzer defocus which is ~ 51 nm for the instrument used, were chosen. The multislice technique was then used to simulate HRTEM images using known values of accelerating voltage, spherical aberration coefficient and other parameters. The atomic displacements in the resulting images were then computed using the GPA technique and compared for qualitative consistency with the initially assumed distortion field.

Using the techniques described above, subject to the limitations and the corresponding precautions adopted, it is of importance to examine the precision and significance of the measurements. Real space measurements of lattice spacing from the HRTEM negatives can be carried out with a precision of 0.01 nm. For measurements in the reciprocal space using peak detection algorithms, precision in real space of better than 1% is achievable. This corresponds to a measurement precision of the order ± 0.003 nm for a hypothetical lattice spacing of 0.3 nm. In the case of GPA, the precision of the results depends on the numerical accuracy of the calculations. This is estimated to be of the order of 0.001 nm. This estimate of the precision obtainable by GPA is consistent with similar estimates in literature. Ade & Lauer (1999) have used the GPA technique on images calculated for a deformed crystal and concluded that the error in the determination of lattice deformations is smaller than 1% of the lattice fringe spacing.

3. Results

Figures 2 a & b show low magnification bright field images and the corresponding electron diffraction patterns. The grain sizes were measured from several bright and dark field images in the range 5.5 to 7.5 nm. The grains are seen to be equiaxed. The diffraction patterns showed rings which could be indexed to face centred cubic structure of palladium. No other phases were detected. Table 1 shows the indexing of the SAD pattern in figure 2b. It is seen that the plane spacings measured from the ring pattern were consistently higher than the bulk palladium 'd' spacing calculated for coarse-grained palladium. These latter values are listed in the third column of table 1.

Figure 3 is a lattice image from the nanocrystalline palladium. Due to the resolution limit of the electron microscope used, predominantly (111) lattice planes which correspond to a

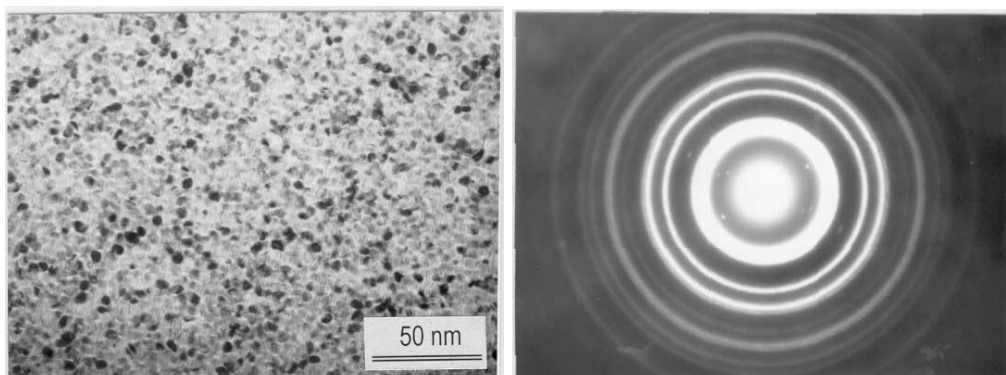
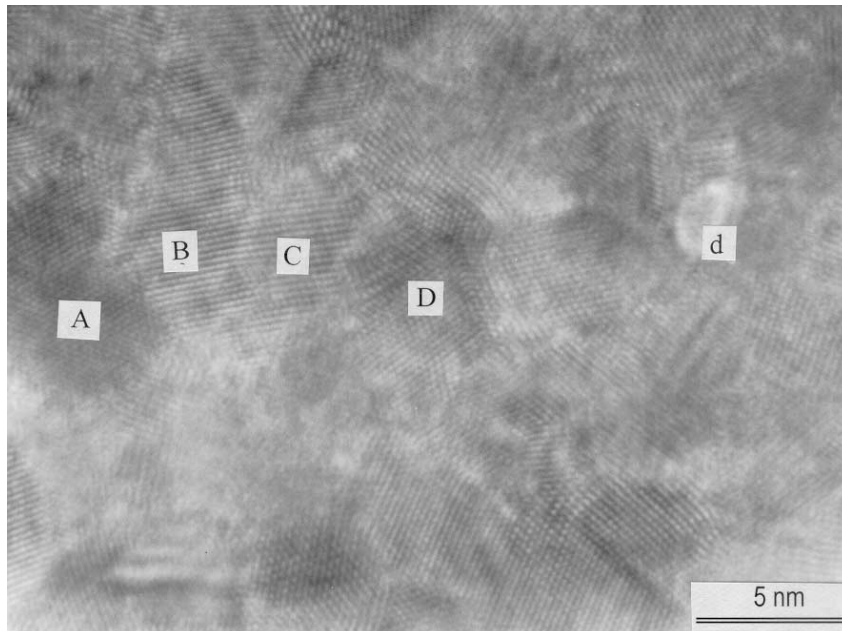


Figure 2. Low magnification bright field image and corresponding selected area electron diffraction pattern from thin film nanocrystalline palladium.

Table 1. Indexing of ring SAD pattern from palladium thin film.

Ring #	d (nm)	Bulk d (nm)	hkl
1	0.243	0.2244	(111)
2	0.208	0.1944	(002)
3	0.149	0.1374	(022)
4	0.125	0.1172	(113)
5	0.121	0.1122	(222)
6	0.107	0.0972	(004)
7	0.097	0.0892	(133)
8	0.094	0.0794	(224)
9	0.085	0.0748	(115)
10	0.081	0.0697	(044)
11	0.070	0.0657	(135)

spacing $d_{(111)} = 0.2244$ nm are imaged. These are seen to be oriented without a preferred direction in the plane of the thin film, throughout the film. The grain interiors are seen to be largely defect free. Moiré effects are seen in a few places where grains overlap in the beam direction. Disordered regions are seen within some grains. A preliminary examination of these regions of disorder of size same as that of the grains by changing the defocus of the objective lens showed that these grains happen to lie at different levels due to the thin film not being

**Figure 3.** HRTEM image showing the various interfacial image features in nanocrystalline palladium.

perfectly flat. Variation in the grain size in the direction of the incident electron beam is another factor that contributes to this effect. A number of twin interfaces are also seen in figure 3.

A closer examination of the grain boundaries between various grains shows that the structure is seen to vary in character in terms of the extent of disorder at the boundary. At grain boundaries such as those between grains 'A' and 'B' little disorder is seen. The lattice planes are seen to extend all the way to the grain boundary in either crystal. Conversely, grain boundary between grains 'C' and 'D' is seen to show disorder to the extent of 1–2 lattice plane spacings. The maximum disorder measured perpendicular to the grain boundary in the foil plane is about 0.5 nm or about two lattice plane spacings.

The two boundaries described above represent structural extremes seen in the system. Many grain boundaries show intermediate character. These boundaries seem to have a varying structure: while some regions of the boundary are sharp, adjacent regions along the same boundary appear disordered. In most such cases, it is seen that a disordered triple-line junction defect lies further along the boundary and the disordering of the grain boundary structure is presumably a result of the triple-line junction relaxation effect.

Regions with brighter contrast (marked 'd') can be seen at many of the grain junctions in figure 3, especially at triple line junctions. These are seen to lack any periodicity within. The bright contrast could be due to voids or alternatively due to disorder at the triple line junctions. To confirm the nature of these regions, defocus experiments were carried out. Figure 4 shows one such series of HRTEM micrographs recorded for the palladium film for the disordered triple line junction image of the type marked 'd' in figure 3. The underfocus relative to figure 4a is indicated in nanometres. It is seen that apart from the Fresnel fringe,

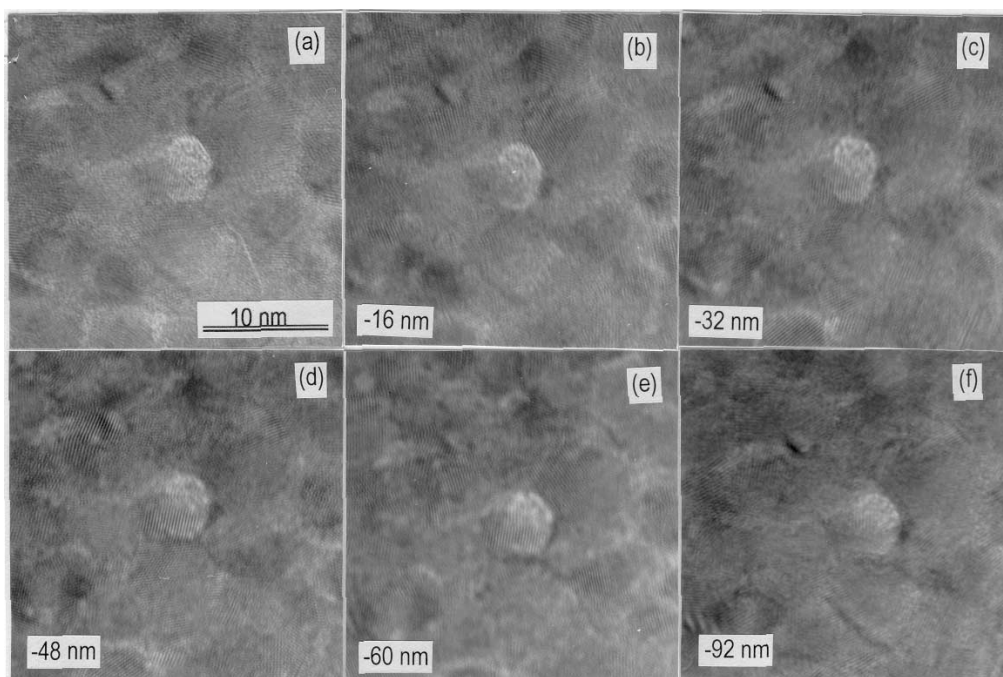


Figure 4. Triple line junction region in a defocus series. The defocus relative to the image (a) is indicated. The observed contrast variation suggests a disordered structure rather than a nanovoid.

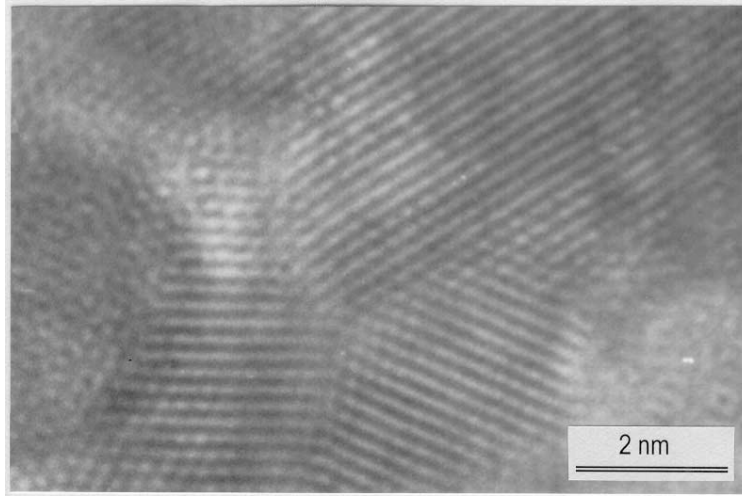


Figure 5. Disorder free triple line junction in nanocrystalline grain in palladium.

residual granular contrast is seen in all the images in the series indicating the presence of disordered material at the triple line junction. This indicates that the bright contrast regions at the triple line junctions represent disordered regions unlike the grain regions that reveal periodicity with change in defocus of the objective lens. However, not all triple line junctions show disorder. Figure 5 is an example of a triple line junction that does not show disorder.

The inter-planar spacing for (111) planes in palladium was found to be 0.24 ± 0.01 nm by measuring directly from the HRTEM negatives and averaging over large number of measurements. Similarly, measurement through the power spectrum yielded a comparable value at 0.238 ± 0.005 nm. These correspond to 4–8% excess over the bulk value of $d_{(111)} = 0.2244$ nm. The lattice spacings show a wide variation among the different grains without any preferred pattern.

Figure 6 shows the results from two sets of simulated images from a distorted lattice for which the result of GPA is superimposed as a quiver plot. The arrows indicate the direction and magnitude of the displacement from the undistorted lattice. The first set in figure 6a shows the effect of variation in the specimen thickness between 8 and 24 nm. The second set in figure 6b shows the effect of variation in defocus between 46 and 56 nm. It is seen that while the image contrast varies considerably in the range of thickness and defocus values, the results of GPA on these images yields qualitatively the same distortion field.

GPA technique applied to experimental HRTEM images of a number of grains of nanocrystalline palladium grains from a number of thin films showed a distribution of displacement vectors. Averaged over a large number of grains the maximum and mean displacement magnitudes are 0.041 nm and 0.013 nm respectively. This represents a scalar average of the atomic displacements in the various directions. Considering the vectorial displacements, which are of more interest and importance, it is seen that the nanocrystallites adjacent to disordered regions either at the interface between two grains or at the triple line junction shows non-uniform distortion fields. The distribution of the displacement field is not uniform across the grain. Rather, the distribution corresponds to the state of relaxation at the interfaces between nanocrystalline grains.

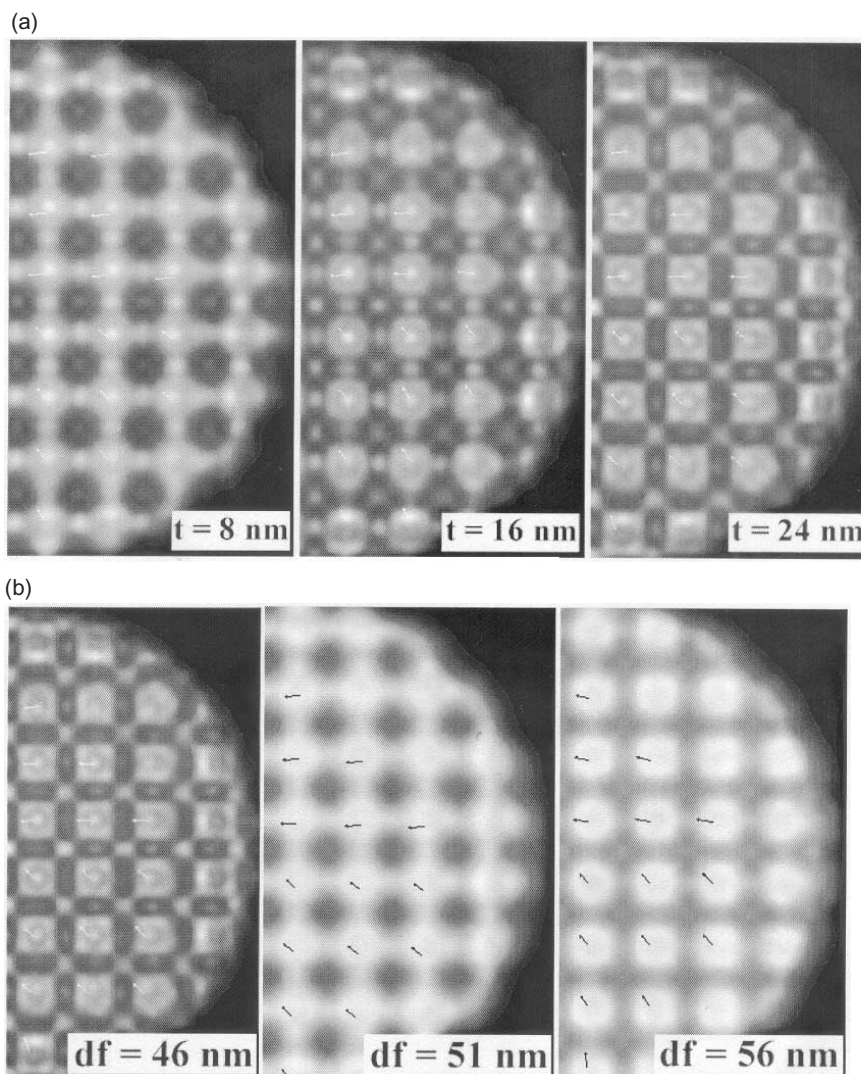


Figure 6. Geometric phase analysis applied to images simulated from a crystal with distortion. (a) $df = 46 \text{ nm}$. (b) $t = 24 \text{ nm}$.

4. Discussion

In the present HRTEM lattice images, many of the triple line junctions in nanocrystalline palladium show brighter contrast over regions 1–2 nm wide. Previous HRTEM studies of nanocrystalline palladium (Wunderlich *et al* 1990; Ping 1995a) have shown bright contrast regions at triple line junctions and interpreted them to be nanovoids. It is important to distinguish between the two possible interpretations of such features, namely nanovoids and disordered regions. The former can occur either because of incomplete coverage in the thin film synthesis, or because of relaxation of the neighbouring grain boundaries. No contrast in the HRTEM image is expected from nanovoids except for Fresnel fringes at high defo-

cus setting of the objective lens. On the other hand, residual contrast is expected at all defocus settings in addition to the Fresnel fringes in the case of disordered regions. Thus, it is possible to distinguish between nanovoids and disordered regions at triple line junctions using a defocus series of images. Figure 4 demonstrates one such exercise in the case of nanocrystalline palladium thin film. In most cases, the bright contrast areas are seen to be disordered regions and correspond to structural disorder at the triple line junctions. The other possibility of nanovoids has been seen only very rarely. Thus, the observed bright contrast regions at many of the triple line junctions can be construed as structurally disordered defects.

The observation of structurally disordered regions at triple line junctions confirms results from positron lifetime spectroscopy technique. Positron lifetimes in a material are inversely proportional to the local electron density. Thus, positron lifetimes are longer at defects where the electron concentration is lower. Positron lifetimes are expected to be longer at disordered regions where the vacancy concentration is higher as in amorphous materials. This technique has been used to probe the structure of nanocrystalline iron, palladium and silver (Schaefer & Würschum 1987; Qin *et al* 1998). In the case of nanocrystalline palladium, the positron lifetime spectra could be deconvoluted to two components. The shorter of these lifetimes is correlated to monovacancy type defects while the other is correlated with vacancy clusters consisting of 10–15 vacancies with a spatial spread estimated to be of the order of 1 nm. This can be correlated to the bright contrast regions seen at the triple line junctions in the HRTEM in terms of the dimensions of the defect. However, as discussed above, detailed analysis in the HRTEM leads to the conclusion of structurally disordered region rather than nanovoids as proposed by Schaefer *et al* (1989) and Qin *et al* (1998). Thus the complementary technique of positron lifetime spectroscopy provides evidence for dimensionally similar defects at interfaces while the detailed analysis from the direct imaging HRTEM technique shows them to be correspond to structural disorder.

The present HRTEM results on the grain boundaries in nanocrystalline thin films show a variety of structures from ordered to that showing significant disorder. Grain boundaries can relax both parallel and perpendicular to the boundary because of the high density of grain boundaries in nanocrystalline materials and their mutual interactions. Due to the limitation of the HRTEM technique whereby relaxation along the incident beam directions cannot be imaged, this can result in grain boundary images that appear to vary in character. However, the experimental evidence reported here does not support a generalised disorder at grain boundaries that could be termed as 'gas-like'. The presence of gas-like disorder would have resulted in HRTEM lattice images that showed significant atomic displacements normal to the grain boundary plane at all grain boundaries including those that appeared ordered. Due to the large fraction of atoms constituting the grain boundaries in nanocrystalline materials, relaxation effects are expected to be very significant. The seemingly contrasting observations of ordered and disordered grain boundaries have to be understood in terms of such relaxation effects rather than as a disorder inherent to the grain boundary structure. This is especially true at the nanocrystalline grain sizes where the grain boundary curvature is high.

Twin interfaces have been observed in all the nanocrystalline systems studied and have been reported to be particularly common in the *fcc* systems as in the case of palladium. In terms of grain boundary energy, these twin boundaries are particularly low energy configurations. This has the consequence that the boundary stability is enhanced. In literature, the occurrence of twinned nanocrystals is reported to be common in physical vapour deposited thin films and in particular, in thin films of face centred cubic noble metals such as silver and gold.

The presence of pentagonal twinning in nanoparticles of face centred cubic noble metals has been reported by many researchers. The resulting pentagonal symmetry is different from that of quasicrystals. In the case of pentagonal twin clusters, five twin boundaries meet at the centre of the nanoparticle. A possible reason for the frequent occurrence in nanocrystalline materials is minimisation of the elastic strain energy (Tehuacanero *et al* 1992) associated with the boundaries and a minimisation of the surface energy of the nanograins.

The role of disclinations gains more importance in nanocrystalline solids owing to the high density of grain boundaries and triple line junctions, and due to the instability of translational defects like dislocation in the nanocrystallites. Formation of amorphous packets is a strong relaxation mode of triple junction disclinations (Gryaznov & Trusov 1993). The amorphous packets represent U-line triple junctions. A non-uniform state of stress should exist in the films because of the varying screening effect of disclinations. This should result in variations in the inter-planar spacings in the different nanograins. Hence the d 'spacings vary randomly in nanocrystalline palladium. Thus, it can be said that each grain is in a different state of elastic stress, which in turn could have an indirect role on the mechanical deformation of the nanocrystalline materials. This also explains the result where it is seen that not all grain junctions contain such amorphous packets.

A consequence of the role of disclinations in nanocrystalline materials as described above is seen in the solid-state amorphisation reaction (SSAR) phenomenon. A crystal to amorphous transition can be considered to be associated with an increase in disclination content in the material. For example, splitting of a triple junction disclination in a nanocrystalline into smaller power partials can lead to the formation of amorphous regions at the core of the initial defects (Osipov & Ovid' Ko 1992). The driving forces for this process are a decrease in elastic energy due to splitting and screening of disclinations and the negative free energy of mixing in SSAR systems. The increase in volume fraction of triple line junctions corresponding to a decrease of grain size (see figure 1) considered along with the disclination structure at triple line junctions suggests a possible mechanism for SSAR. Based on this, the SSAR process can be visualised as a continuous transformation to successively smaller grain sizes eventually resulting in the amorphous phase with the triple line junctions serving as heterogeneous nucleation sites for the amorphous phase. Experimental support for this argument is seen in the case of Al-Ge system. TEM study of annealed Al-Ge bilayers (Raghavan *et al* 1998) has shown the amorphous phase to nucleate in the interfacial regions and the SSAR to proceed via the progressive breakdown of the nanocrystalline grains into smaller grains. From the presence of interfacial features in nanocrystalline materials that are desirable for SSAR as discussed above, it has been suggested that the nanocrystalline state is an essential precursor to solid state amorphisation (Sundararaman 1995).

The GPA technique is applied for the first time to the analysis of lattice disorder in nanocrystalline materials. In this sense, the present work is a preliminary report on the potential information that can be quantified in HRTEM images of this class of materials. Hence, it is important to consider the various factors that affect the relevance and accuracy of the results obtained by this technique. The primary requirement for a successful application of the GPA technique is that the phases derived from the HRTEM images should be a true representation of the specimen structure including the defects under study. Ade & Lauer (1999) have presented a theoretical analysis of the applicability of GPA method to the quantification of lattice distortions from HRTEM images. This analysis has validated the technique provided that the thickness of the specimen does not vary significantly across the image and that the distortion field is slowly varying. An additional simplifying assumption made is that of coherent illumination. In the present case of nanocrystalline materials, the former two requirements with

regard to specimen thickness variation and slowly varying deformation are met when HRTEM images from nanocrystalline grains are considered. In a strict sense the assumption of coherent illumination is satisfied only for images recorded with illumination from a field emission gun. The present experimental images however, have been recorded with illumination from a LaB6 filament. There is a need for a detailed analytical examination of the technique that includes the effect of a partially coherent illumination. On the other hand, the results of the simulations presented in figure 6 show that over a small domain in the foil thickness - defocus space, GPA yields reproducible results that can be correlated to the assumed distortion field. This lends support to the use of the technique for the measurement of lattice distortions in these materials. Further, it is seen that the displacements measured within nanocrystalline grains are not concentrated either at the grain boundaries or at the centre of the grain. Rather, the geometrical distribution of these displacements is indicative of the relaxation mode of the nanocrystallites in consonance with the interfacial component of the nanocrystalline phase.

In literature, it has been proposed that the lattice expansion of nanocrystalline materials is because of the higher equilibrium solubility of vacancies. However, this should result in a displacement field that is isotropic. Other HRTEM studies have indicated that the lattice expansion should be close to the interface while the intra-grain region being essentially strain free. The present results directly link the distortion within the nanocrystallites to the adjacent interface structure. As seen from the present results, the effect of the interface structure is also seen on the crystal lattice of the phase when the grain size reduces to nanometre levels. Presumably, at still smaller grain sizes, where the curvature of the grain boundaries is further enhanced, effect of the interface structure on the crystal lattice is further enhanced leading to higher distortions. It is further worth considering our results in the light of the proposed 'gas-like' disorder of Gleiter and co-workers. An interfacial disorder of the kind proposed by these researchers would presumably have resulted in an isotropic distribution of the displacements. However, our results linking the interfacial disorder and the crystal lattice disorder deny the existence of uniformly disordered grain boundaries. Nevertheless, the importance of the measured atomic displacements lies in the possible linkage to interfacial properties such as the excess free volume of grain boundaries. Recently, in analysing the impact of grain boundaries on thermodynamic equilibrium, Weissmüller (2001) has postulated that the strain in nanocrystalline grains is intrinsic to this class of materials. The strain is said to arise due to accommodation of an integral number of lattice planes in the space bounded by other nanocrystalline grains in the case of a fully dense nanocrystalline material. Empirical relations have been developed to relate the quantum of strain to the grain size and subsequently to the interfacial energy. The analysis technique used in the present work needs to be extended to verify such relations or alternatively to evolve a methodology for determining grain boundary properties.

5. Conclusions

Grain boundaries show disorder that can be related to the relaxation effects in nanocrystalline materials. However, no evidence for 'gas-like' disorder is found. The observed structural characteristics of interfaces in nanocrystalline materials involve interplay between the grain boundaries and triple line junctions. The two structural constituents together determine interface structures that result in nanocrystalline materials. The disclination model can provide a link between the two major constituents of interfaces in nanocrystalline materials, namely,

the grain boundaries and the triple line junctions. The varying degrees of relaxation of disclinations in nanostructured materials can lead to a variety of grain boundary structures and are also responsible for the random variation in its lattice parameter in the different nanocrystalline grains. Geometrical phase analysis has been used to measure atomic displacement fields in HRTEM images of nanocrystalline grains. It is inferred from the non-uniformity of the displacement distributions that there is no case for disorder localised at the interfaces. Instead, the crystalline component of nanocrystalline materials has to be considered in consonance with the interface component. As an extension of the present work, it is of interest to examine the relation between the measured strain and interfacial properties.

One of the authors (RD) would like to acknowledge guidance received from Prof. S Ranganathan, Indian Institute of Science and from Shri E Mohandas during the course of the above research. Encouragement and support from Dr Baldev Raj is also gratefully acknowledged.

References

- Ade G, Lauer R 1999 Direct determination of lattice distortions by digital processing of HRTEM images of crystals. *Ultramicroscopy* 77: 177–185
- Arzt E 1998 Size effects in materials due to microstructural and dimensional constraints: A comparative review. *Acta Mater.* 46: 5611–5626
- Bollmann W 1988 Triple-line disclinations - representations, continuity and reactions. *Philos. Mag.* A57: 637–649
- Crozier P A, Tsen S C Y, Liu J, Cortes C L, Perez-Omil J A 1999 Factors affecting the accuracy of lattice spacing determined by HREM in nanometre sized Pt particles. *J. Electron Microsc.* 48: 1015–1024
- Divakar R, Raghunathan V S, Ranganathan S 2001 Image analysis for high resolution transmission electron microscopy. *Image analysis in materials and life sciences* (eds) C Babu Rao, P Kalyanasundaram, K K Ray, Baldev Raj (Oxford & IBH) pp 73–79
- Eastman J A, Fitzsimmons M R, Müller-Stach M, Wallner G, Elam W T 1992 Characterisation of nanocrystalline palladium by x-ray diffraction and EXAFS. *Nanostruct. Mater.* 1: 47–52
- Feynman R P 1960 There's plenty of room at the bottom - An invitation to enter a new field of physics. *Eng. Sci.* at <http://www.zyvex.com/nanotech/feynman.html>
- Fitzsimmons M R, Eastman J A, Müller-Stach M, Wallner G 1991 Structural characterization of nanometer-sized crystalline Pd by X-ray-diffraction techniques. *Phys. Rev.* B44: 2452–2460
- Gleiter H 2000 Nanostructured materials: basic concepts and microstructure. *Acta Mater.* 48: 1–29
- Gryaznov V G, Trusov L I 1993 Size effects in micromechanics of nanocrystals. *Prog. Mater. Sci.* 37: 289–401
- Haubold T, Birringer R, Lengeler B, Gleiter H 1989 EXAFS studies of nanocrystalline materials exhibiting a new solid state structure with randomly arranged atoms. *Phys. Lett.* A135: 461–466
- Lengeler B, Eisenberger P 1980 Extended X-ray absorption fine structure analysis of interatomic distances, co-ordination numbers and mean relative displacements in disordered alloys. *Phys. Rev.* B21: 4507–4520
- Li D X, Ping D H, Ye H Q, Qin X Y, Wu X J 1993 HRTEM study of the microstructure in nanocrystalline materials. *Mater. Lett.* 18: 29–34
- Löffler J F, Wagner W, Kostorz G 2000 Grain-size dependence of intergranular magnetic correlations in nanostructured metals. *J. Appl. Crystallogr.* 33: 451–455
- Malm J O, O'Keefe M A 1997 Deceptive "lattice spacings" in high resolution micrographs of metal nanoparticles. *Ultramicroscopy* 68: 13–23

- Melmed A J, Hayward D O 1959 On the occurrence of fivefold rotational symmetry in metal whiskers. *J. Chem. Phys.* 31: 545–546
- Mills M J 1993 High-resolution transmission electron microscopy and atomistic calculations of grain boundaries in metals and intermetallics. *Mater. Sci. Eng.* A166: 35–50
- Nieh T G, Wadsworth J 1991 Hall–Petch relation in nanocrystalline solids. *Scr. Metall.* 25: 955–958
- Osipov A V, Ovid'ko I A 1992 Diffusion induced decay of disclinations and solid state amorphisation in mechanically alloyed materials. *Appl. Phys.* A54: 517–519
- Palumbo G, Thorpe S J, Aust K T 1990 On the contribution of triple junctions to the structure and properties of nanocrystalline materials. *Scr. Metall.* 24: 1347–1350
- Ping D H, Li D X, Ye H Q 1995 HRTEM study on the microstructure of nanocrystalline materials. *Proc. 6th Beijing Conf. and Exhibition on Instrum. Analysis*, pp A75–A76
- Ping D H, Li D X, Ye H Q 1995 Microstructural characterization of nanocrystalline materials. *J. Mater. Sci. Lett.* 14: 1536–1540
- Qin X Y, Zhu J S, Zhang L D, Zhang X Y 1998 Formation process of interfaces and microdefects in nanostructured Ag studied by positron lifetime spectroscopy. *J. Phys.* 10: 3075–3088
- Ranganathan S, Divakar R, Raghunathan V S 2000 Interface structures in nanocrystalline materials. *Scr. Mater.* 44: 1169–1174
- Raghavan G, Divakar R, Tripura Sundari S, Sundararaman D, Tyagi A K, Kanwar Krishan 1998 Heterogeneous nucleation of the amorphous phase and dissolution of nanocrystalline grains in bilayer Al-Ge thin films. *Scr. Mater.* 38: 59–65
- Schaefer H E, Würschum R 1987 Positron lifetime spectroscopy in nanocrystalline iron. *Phys. Lett.* A119: 370–374
- Schwoebel R L 1966 Anomalous growth of gold from the vapor phase. *J. Appl. Phys.* 37: 2515–2516
- Stadelmann P A 1987 EMS - A software package for electron diffraction analysis and HREM image simulation in materials science. *Ultramicroscopy* 21: 131–146
- Sundararaman D 1995 Nanocrystalline state and solid state amorphization. *Mater. Sci. Engg.* B33: 307–313
- Tehuacanero S, Herrera R, Avalos M, Yacamàn M J 1992 High resolution TEM studies of gold and palladium nanoparticles. *Acta Metall.* 40: 1663–1674
- Thomas G J, Siegel R W, Eastman J A 1990 Grain boundaries in nanocrystalline palladium: High resolution electron microscopy and image simulations. *Scr. Metall. Mater.* 24: 201–206
- Weissmüller J 2000 Grain boundaries and their impact on thermodynamic equilibrium. *Science of metastable and nanocrystalline alloys. Structure, properties and modelling* (eds) A R Dinesen, M Eldrup, D J Jensen, S Linderoth, T B Pederson, N H Pryds, A Schrøder, J A Wert (Denmark: Risø Nat. Lab.)
- Wood G J, Stobbs W M, Smith D J 1984 Methods for the measurement of rigid body displacements at edge-on boundaries using high resolution electron microscopy. *Philos. Mag.* A50: 375–391
- Wunderlich W, Ishida Y, Maurer R 1990 HRTEM studies of the microstructure of nanocrystalline palladium. *Scr. Metall. Mater.* 24: 403–408
- Zhu X, Birringer R, Kerr U, Gleiter H 1987 X-ray diffraction studies of the structure of nanometer-sized crystalline materials. *Phys. Rev.* B35: 9085–9090